Leukemia & Lymphoma Society. M.-A.H. was supported by a postdoctoral fellowship from Association pour la Recherche sur le Cancer (FRANCE). D.A.B. is a recipient of an NIH training grant.

Competing interests statement

The authors declare that they have no competing financial interests.

Correspondence and requests for materials should be addressed to R.S. (e-mail: shiekhattar@wistar.upenn.edu).

Reverse engineering of the giant muscle protein titin

Hongbin Li*, Wolfgang A. Linke†, Andres F. Oberhauser*, Mariano Carrion-Vazquez*, Jason G. Kerkvliet*, Hui Lu‡, Piotr E. Marszalek* & Julio M. Fernandez*

** Department of Physiology and Biophysics, Mayo Foundation, Rochester, Minnesota 55905, USA*
† Institute of Physiology and Pathophysiology, University of Heidelberg, D-69120 Heidelberg, Germany
‡ Donald Danforth Plant Science Center, St Louis, Missouri 63132, USA

Through the study of single molecules it has become possible to explain the function of many of the complex molecular assemblies found in cells[1–5]. The protein titin provides muscle with its passive elasticity. Each titin molecule extends over half a sarcomere, and its extensibility has been studied both *in situ*[6–10] and at the level of single molecules[11–14]. These studies suggested that titin is not a simple entropic spring but has a complex structure-dependent elasticity. Here we use protein engineering and single-molecule atomic force microscopy[15] to examine the mechanical components that form the elastic region of human cardiac titin[16,17]. We show that when these mechanical elements are combined, they explain the macroscopic behaviour of titin in intact muscle[6]. Our studies show the functional reconstitution of a protein from the sum of its parts.

Individual titin molecules span both the A-band and I-band regions of muscle sarcomeres. The I-band part of titin has been identified as the region that is functionally elastic. We study the shortest titin isoform, the N2B isoform found in cardiac-muscle sarcomeres. The elastic I-band region of N2B-titin can be subdivided into four structurally distinct regions (Fig. 1): a proximal immunoglobulin region containing 15 tandem immunoglobulin-like (Ig) domains; a middle N2B segment that contains a 572-residue amino-acid sequence of unknown structure; a 186-amino-acid-long segment rich in proline (P), glutamate (E), valine (V) and lysine (K) residues, named the PEVK region; and a distal Ig region that contains 22 tandem Ig modules[17]. We use polyprotein engineering[18,19] and single-molecule force spectroscopy to dissect the individual mechanical elements of the I-band of cardiac titin and reconstruct the elasticity of cardiac muscle. Polyproteins, when mechanically stretched by single-molecule atomic force microscopy (AFM) give distinctive mechanical fingerprints as their modules unfold sequentially (sawtooth patterns in the force–extension curve)[18], and can be used to positively identify the mechanical features of a single molecule[19–21] (Supplementary Information).

The top trace in Fig. 1a shows a typical sawtooth pattern measured by stretching a protein composed of eight modules from the proximal tandem Ig region, I4 to I11. The sawtooth pattern shows that all modules unfold in the range of 150–200 pN. However, there is a slight tendency for the first unfolding event to occur at a lower force than later unfolding events. In order to examine this tendency, we plot the average value of all first unfolding peaks, second peaks, and so on (Fig. 1b, filled circles). A linear fit to the data (Fig. 1b, thin line through filled circles) showed only a weak hierarchy of 12 pN per force peak. Polyproteins constructed using modules I4 ($I4_8$) and I5 ($I5_8$) showed similar unfolding forces of 150–200 pN (Fig. 1b, open circles). Hence, it seems that the proximal tandem Ig region has modules of similar mechanical stability. We studied the I4 polyprotein in more detail following the AFM protocols of ref. 18, and measured an unfolding rate of $3 \times 10^{-3}\,s^{-1}$ and a folding rate of $0.33\,s^{-1}$.

Similar experiments done with polyproteins from the distal Ig region revealed a very different picture. Stretching a protein composed of eight modules from the distal tandem Ig region, I27 to I34, showed a much broader range of unfolding forces, from ~150 pN up to 330 pN (Fig. 1a, bottom trace). As before, we plot the average value of all first unfolding peaks, second peaks, and so on (Fig. 1b, filled squares). A linear fit to the data (Fig. 1b, thin line through

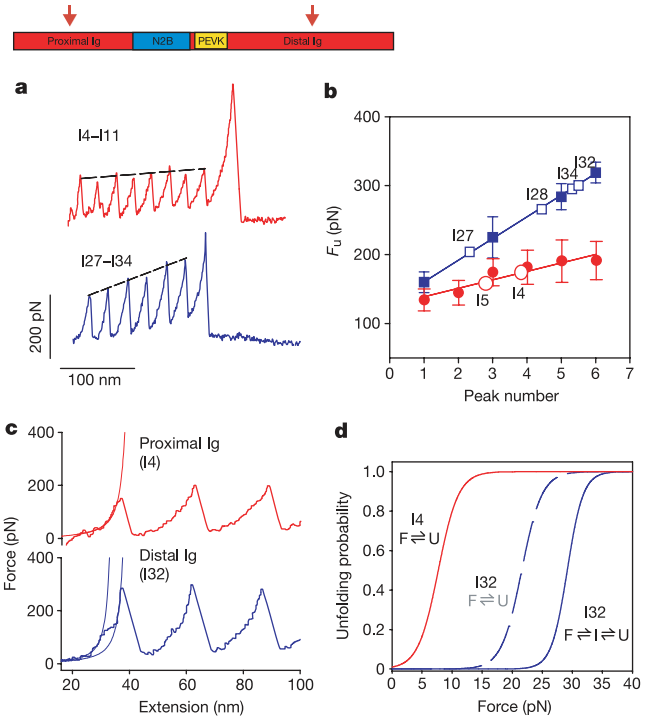

Figure 1 The proximal and distal tandem Ig regions of cardiac titin have different mechanical properties. Inset, the structurally distinct elements of I-band titin. The arrows point to the tandem Ig regions. **a**, Top trace: force–extension curve obtained from an engineered protein comprising domains I4 to I11 of the proximal tandem Ig region. Bottom trace: force–extension curve obtained from a protein comprising domains I27 to I34 of the distal tandem Ig region. **b**, Unfolding forces (F_u) measured for consecutive unfolding peaks (1–6) in AFM recordings of the I4–I11 protein (filled circles) and the I27–I34 protein (filled squares). Recordings obtained from polyproteins containing only I27, I28, I32, or I34 Ig domains (open squares; $I27_8$: 204 ± 26 pN, $n = 266$; $I28_8$: 257 ± 27 pN, $n = 245$; $I34_8$: 281 ± 44 pN, $n = 32$; $I32_8$: 298 ± 24 pN, $n = 132$) show a strong hierarchy. The stability of I4 and I5 polyproteins (open circles, $I4_8$ and $I5_8$; I4: 171 ± 26 pN, $n = 136$; I5: 155 ± 33 pN, $n = 196$) confirms the weak hierarchy of the proximal region. **c**, Top trace: force–extension relationship of an I4 polyprotein ($I4_8$). The initial part of the force trace, before the first unfolding peak, is well described by the WLC model (thin line). Bottom trace: force–extension relationship for an I32 polyprotein ($I32_8$) from the distal tandem Ig region of titin. In the initial rising phase of the force–extension curve, a prominent 'hump' appears, indicating the presence of an unfolding intermediate[24]. **d**, Plot of the steady-state unfolding probability of the I4 and I32 modules as a function of force. I4 is calculated as a simple two-state unfolding system (solid red line). The I32 module is calculated both in the presence (solid blue line) and in the absence (dashed blue line) of the unfolding intermediate.

filled squares) gave a slope of 31.5 pN per force peak. These results indicate a mechanical hierarchy among these modules. In order to determine the mechanical stability of the individual modules and their ordering in the hierarchical unfolding, we constructed several polyproteins: $I27_8$, $I28_8$, $I32_8$ and $I34_8$. The average unfolding forces were found to be 204 pN for I27 (ref. 18), 257 pN for I28 (ref. 19), 298 ± 24 pN ($n = 132$) for I32 and 281 ± 44 pN ($n = 32$) for I34 (Fig. 1b, open squares). These results contrast with those for the proximal region where no obvious mechanical hierarchy was observed.

Several models of polymer elasticity have been developed to predict the mechanical behaviour of a polymer. As before, we use the worm-like chain (WLC)[22] model to fit the force–extension curves of a polyprotein[18]. A close examination of the force–extension curve obtained from a proximal Ig module ($I4_8$, Fig. 1c) shows that the WLC model fits well the force–extension curve preceding each unfolding event (thin red line in Fig. 1c). The unfolding event that occurs is an all-or-none process that can be easily described by a two-state model of the type F ⇔ U with rate constants for unfolding, $\alpha_u(F)$, and folding, $\beta_f(F)$, that are force dependent[23]. Under a constant force F, the probability of unfolding is given by $P_u(F) = \alpha/(\alpha+\beta)$, which has a sigmoidal shape when plotted against the stretching force (Fig. 1d). The plot shows that for I4, $P_u(F) = 0.5$ at a force of 7.7 pN. This result is similar for I5, and is likely to be similar for the other modules of the proximal Ig region.

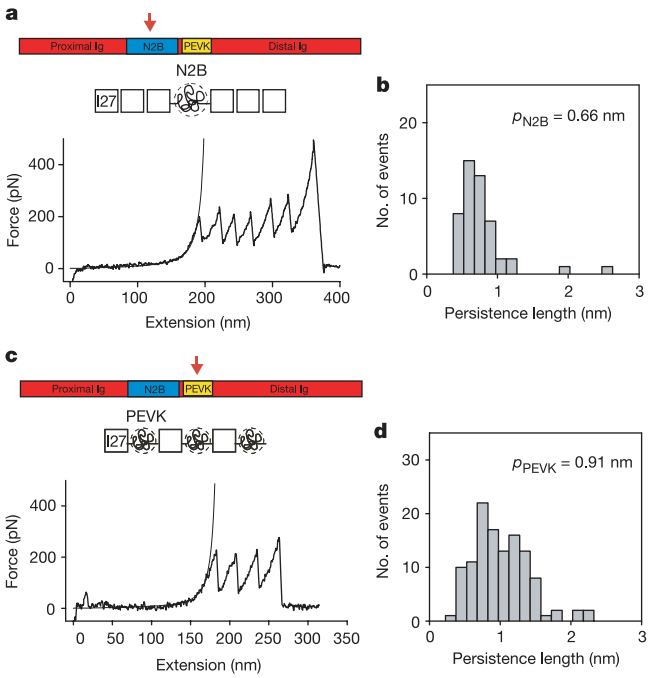

Figure 2 Single-molecule AFM measurements of the mechanical properties of the N2B and PEVK regions of titin. **a**, Top inset: the arrow points to the location of the N213 region in the I-band. Force–extension curve of a protein chimaera containing the cardiac N2B unique sequence flanked on either side by three I27 domains ($I27_3$-N2B-$I27_3$), bottom insert. A Levenberg–Marquardt fit of the WLC equation (thin line) to the force–extension curve before the first I27 unfolding event measured the contour length, L_c, and persistence length, p, of N2B. **b**, Frequency histogram of persistence-length values. A narrow distribution is found, centred at 0.66 nm. **c**, Top inset: the arrow points to the location of the PEVK region in the I-band. Force–extension curve of a protein chimaera containing human cardiac PEVK domains alternating with Ig I27 domains, $(I27\text{-}PEVK)_3$, bottom insert. As in **a**, we used Levenberg–Marquardt fits of the WLC equation to measure L_c and p of the PEVK region (thin line). **d**, Frequency histogram of persistence-length values measured for the PEVK domain. A relatively broad distribution is seen ($p = 0.4$–2.5 nm; average value, 0.91 nm).

The WLC model does not fit the force–extension curve of the I32 polyprotein (Fig. 1c, bottom trace) because of a pronounced 'hump' that corresponds to an unfolding intermediate before full unfolding[24]. We have observed a similar intermediate in all of the distal Ig modules tested, whereas we have not observed such an intermediate in the proximal domains. This unfolding intermediate may serve as a kinetic trap to stabilize the distal domains and protect them against unfolding. To illustrate this point, we first ignore the unfolding intermediate, and consider a simple two-state unfolding reaction with $P_u(F) = \alpha/(\alpha+\beta)$. The rate constants, α and β, are calculated from the peak unfolding forces and their dependence on the rate of stretching[18], ignoring the unfolding intermediate. Figure 1d (dashed line) shows that $P_u(F) = 0.5$ at 21.6 pN for I32 in the absence of an unfolding intermediate. When the intermediate is considered, we use a simplified three-state model like F ⇔ I ⇔ U. Two sets of rate constants describe this model: α_u and β_u corresponding to the main unfolding reaction taken to occur between the intermediate and the unfolded state, and α_I and β_I describing the forward and backward rates of transition to the intermediate state. These last two rate constants were estimated from the data obtained for the intermediate unfolding state of the I27 module[24]. The unfolding probability for the three-state model is given by:

$$P_u^I(F) = \frac{\alpha_I \alpha_u}{\alpha_I \alpha_u + \beta_I \beta_u + \alpha_I \beta_u} \quad (1)$$

The three-state unfolding probability is a sigmoidal function that is shifted to the right of that calculated without the unfolding intermediate. In this case, $P_u^I = 0.5$ at 29.2 pN. As the on-rate of the unfolding intermediate $\beta_I = 100\ s^{-1}$ is much faster than the off-rate of the main unfolding event $\alpha_u = 0.01\ s^{-1}$, the module under force will not go directly to the unfolded state but rather go back to the folded state. Thus, this unfolding intermediate acts as an absorbing state (or buffering state) that kinetically prevents the module from unfolding. This difference in mechanical stability between distal and proximal Ig domains reflects the mechanical topology of these two classes of Ig modules (Supplementary Information).

In order to study the mechanical properties of the N2B segment, we constructed a polyprotein composed of a single N2B module

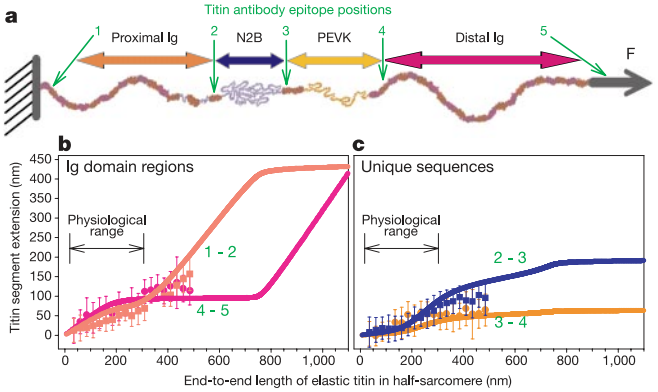

Figure 3 Single-molecule data explain the extensibility of the individual titin segments measured *in situ*. **a**, Schematic diagram showing the four main segments that contribute to the elasticity of titin in the half-sarcomere of cardiac muscle (horizontal arrows). Numbers 1–5 indicate the epitope positions of titin antibodies used to measure the extension of these segments *in situ*[6]. The epitopes move relative to one another when the muscle fibres are stretched. **b**, **c**, Extension of the individual titin segments plotted as a function of the end-to-end extension of I-band titin (symbols). The solid lines were calculated using equations (3)–(5), and the single-molecule data from Table 1. The numbers label the extension of the corresponding epitopes marking the proximal (1–2) and distal (4–5) Ig-domain regions, the N2B unique sequence (2–3) and the PEVK domain (3–4).

Table 1 **Mechanical parameters describing the I-band region of human cardiac titin.**

	Unfolding rate α (s^{-1})	Folding rate β (s^{-1})	Persistence length p (nm)	Kuhn length l_k (nm)	Unfolding distance Δx_u (nm)	Folding distance Δx_f (nm)
Proximal Ig domains	$\alpha_u = 3.3 \times 10^{-3}$	$\beta_u = 0.33$	10 (folded) 0.66 (unfolded)	20 (folded) 1.32 (unfolded)	0.25	2.2
N2B unique sequence	–	–	0.66	1.32	–	–
PEVK segment	–	–	0.91	1.82	–	–
Distal Ig domains	$\alpha_u = 8 \times 10^{-5}$	$\beta_u = 1.2$	10 (folded) 0.66 (unfolded)	20 (folded) 1.32 (unfolded)	0.25	2.2
Unfolding intermediate (I), distal Ig domains	$\alpha_I = 1.0 \times 10^{-2}$	$\beta_I = 10^2$	–	–	0.33	0.33

All values were obtained from single molecule force spectroscopy measurements, except for the persistence length of the folded Ig-domain regions, which was measured from EM images (Supplementary Information).

flanked on either side by three tandem I27 domains ($I27_3$-N2B-$I27_3$; Fig. 2a), where the I27 modules are used to create a mechanical fingerprint. We used single-molecule AFM to obtain force–extension curves from this polyprotein. We collected 48 recordings like the one in Fig. 2a showing a long initial region, without any unfolding peaks, followed by a sawtooth pattern with four to six consecutive unfolding events. The observed unfolding peaks of ~200 pN spaced by ~28 nm correspond to the characteristic fingerprint of the I27 module[18–21]. If we observe at least four I27 unfolding events, then N2B must have been stretched when pulling this protein. Given that the extension of the segments of the protein will be hierarchical, from least stable to most stable[19,20], the long but featureless part of the trace preceding the sawtooth pattern must correspond to the extension of N2B. Then, extension of N2B occurs at low force and without significant energy barriers limiting its extensibility. This result suggests that the N2B segment has the mechanical properties of a random coil.

The WLC model (thin line, Fig. 2a) fits the force–extension curve of N2B and measures a contour length of 209 nm and a persistence length of $p = 0.74$ nm. Similar measurements made in 48 different recordings gave a distribution of persistence lengths that averaged $p_{N2B} = 0.66$ nm (Fig. 2b). We also measured an average contour length of 232 nm, which agrees well with the expected length of a 572-amino-acid-long polypeptide. We also constructed a polyprotein made of three repeats of the dimer PEVK-I27 (Fig. 2c, ref. 20). WLC fits to the force–extension curve of PEVK (thin line, Fig. 2c) measured an average contour length of 68 nm per PEVK segment[20]. The persistence length of PEVK varied from 0.4 nm up to 2.5 nm with an average value of $p_{PEVK} = 0.91$ nm (Fig. 2d, ref. 20), suggesting that PEVK could show mechanical conformations that, while still corresponding to a random coil, had different flexibility.

The extensibility of each elastic segment of cardiac I-band titin has been measured in intact cardiac muscle fibres[6,25], by following the relative position of several sequence-specific titin antibodies (Fig. 3a). We reconstituted the extensibility of I-band titin by calculating the extension of each segment (proximal Ig, N2B, PEVK, distal Ig) at a given force, and repeating this calculation for a range of forces from 0 up to 40 pN. As all segments experience the same force at all times, the segments extend independently of each other and thus their contributions to the overall length are additive. The total end-to-end length of I-band titin, $x(F)_{I\text{-band}}$, is then calculated as the sum of the extension of all segments. The extensibility of a segment has two components: the entropic spring behaviour and module unfolding, if any[11–13].

The N2B and PEVK segments are entropic springs that do not show any unfolding events. These segments are simply modelled by the WLC approach, although with different persistence lengths (we use the average persistence length in each case; $p_{N2B} = 0.66$ nm and $p_{PEVK} = 0.91$ nm). However, the use of the WLC model in this reconstruction is inconvenient, because it gives the force that results from a given extension, $F(x)$, whereas we want to calculate the extension that results from an applied force. The freely jointed chain model of polymer elasticity[26] is described by equation (2).

$$x_{FJC}(F) = L_c u\left(\frac{Fl_k}{k_B T}\right) \quad (2)$$

where L_c is the contour length, $u(Fl_k/k_BT)$ is the Langevin function (where K_B is the Boltzmann constant) and where the Kuhn length $l_k = 2p$ (ref. 22). We can now calculate the extension of these segments for a given force: $x(F)_{N2B}$ and $x(F)_{PEVK}$.

The extensibility of the proximal and distal tandem Ig domain segments, $x(F)_{proximal}$ and $x(F)_{distal}$, is also described by equation (2). However, in this case, L_c and l_k depend on module unfolding (Supplementary Information). Thus, the extension of the proximal Ig region under an applied force, $x(F)_{proximal}$, is fully described by the following three equations:

$$x(F)_{proximal} = L_c^{folded}(F) u\left(\frac{Fl_k^{folded}}{k_B T}\right) + L_c^{unfolded}(F) u\left(\frac{Fl_k^{unfolded}}{k_B T}\right) \quad (3)$$

$$L_c^{folded}(F) = N(1 - P_u(F))4.4 \quad (4)$$

$$L_c^{unfolded}(F) = NP_u(F)32.5 \quad (5)$$

where N is the total number of Ig modules in the segment and $P_u(F)$ is the probability of unfolding at a given force; equations (4) and (5) give lengths in units of nm. The extension of $x(F)_{distal}$ is calculated similarly but including a term for the contribution of the unfolding intermediate. We now calculate the total extension of I-band titin as:

$$x(F)_{I\text{-band}} = x(F)_{proximal} + x(F)_{N2B} + x(F)_{PEVK} + x(F)_{distal} \quad (6)$$

for forces ranging from 0 to 40 pN. This calculation creates a table of values relating $x(F)_{I\text{-band}}$ with $x(F)_{proximal}$, $x(F)_{N2B}$, $x(F)_{PEVK}$ and $x(F)_{distal}$. We can now compare the extensibility of each I-band titin segment with the extensibility measured *in situ*. The parameters used such as the values of persistence length and the unfolding/folding rate constants correspond to the experimentally determined values listed in Table 1. There are no free parameters in this computation.

Figure 3b compares the extensibility of the tandem Ig regions (proximal, orange line; distal, violet line), calculated with equation (6), with their *in situ* extensibility (symbols). The calculated extensibility of these segments agrees well with the myofibril data. The proximal domains extend first in a fully folded configuration. Unfolding of the proximal region becomes obvious at $x(F)_{I\text{-band}} > 300$ nm, whereas unfolding of the distal Ig region does not occur until much later at $x(F)_{I\text{-band}} > 800$ nm. Hence, the single-molecule data predict that in the physiological range ($0 < x(F)_{I\text{-band}} < 300$ nm) the distal Ig region will never unfold any of its modules whereas the proximal region may see a few of its modules unfold towards the high end of the physiological range. Figure 3c shows plots of $x(F)_{N2B}$ (blue line) and of $x(F)_{PEVK}$ (orange line) versus the end-to-end length of the I-band titin, $x(F)_{I\text{-band}}$. The figure shows

that the calculated extension of these segments fits those measured *in situ* (symbols).

Figure 4 plots the relationship between force and the end-to-end length of I-band titin, $x(F)_{\text{I-band}}$ calculated from equation (6) (solid red line). We compare this calculation with the passive force versus sarcomere length relationship of an intact cardiac myofibril[6] measured under quasi-steady-state conditions (no viscous or viscoelastic forces present)[6,27]. The filled symbols in Fig. 4 correspond to single cardiac myofibril data scaled by the number of titin molecules per cross-sectional area of muscle (assumed to be 6×10^9 titin molecules per mm^2)[28]. The figure shows that the force–extension relationship calculated from the single-molecule AFM data faithfully predicts the force–extension relationship measured in intact myofibrils. So by scaling the single-molecule data, it is possible to reproduce the passive elasticity of an intact myofibril. A similar reconstruction can also be done by numerically inverting the WLC model of polymer elasticity (Supplementary Information).

The physiological range of sarcomere lengths for a cardiac myofibril is 1.8–2.4 μm (ref. 29), corresponding to an extension range of 0–300 nm for I-band titin. The single-molecule data show that at an extension of 300 nm, the force reaches ~4 pN per I-band titin molecule. This force is about the same as that generated by a single myosin molecule[4]. At this force, the unfolding probability of the proximal tandem Ig region is low, $P_u = 0.1$. By contrast, the unfolding probability of the distal region is six orders of magnitude smaller. These results show that towards the end of the physiological range, unfolding of a few proximal Ig domains is possible whereas the distal domains always remain folded. If the unfolding probability of the proximal and distal Ig regions was zero, we would observe a purely entropic force–extension relationship (Fig. 4, black line). A purely entropic mechanism explains most of the extensibility of I-band titin in the physiological range, however, it departs significantly at higher extensions. These results suggest that unfolding of the proximal tandem Ig region may serve as a buffer to protect cardiac sarcomeres from developing damaging high forces. This becomes clear if we compare the effects of an over-extension to 450 nm. I-band titin will respond by unfolding several proximal Ig domains, limiting the force to ~7 pN. By contrast, if unfolding were not possible, the force developed would exceed 40 pN per molecule, probably damaging sarcomeric structures. □

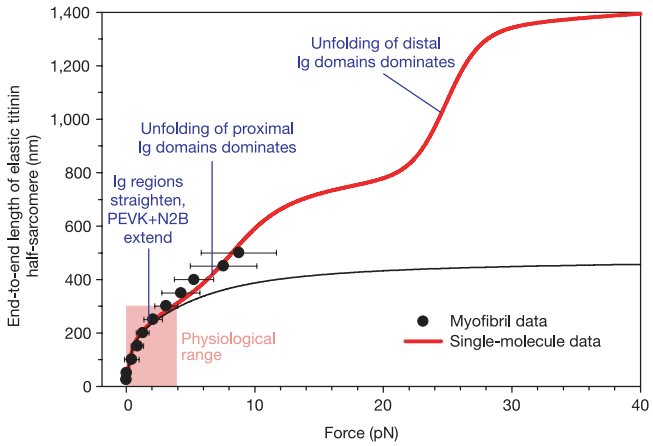

Figure 4 Single-molecule data predict the force–extension curve of cardiac muscle. The red line red plots the calculated (equation (6)) end-to-end length of I-band titin versus a stretching force. The black line also plots equation (6), but in this case the unfolding probability of both the proximal and distal tandem Ig regions was set to zero. The symbols plot force–extension measurements from non-activated rabbit cardiac myofibrils. The values of the measured force were scaled to a single molecule assuming 6×10^9 titin molecules per mm^2 of cross-sectional area. The data show that the single-molecule data fully explain the force–extension relationship within and beyond the physiological range (coloured box).

Methods

Protein engineering

All constructs were from human cardiac titin[16,17]. Titin modules I4–I11, I4, I5, PEVK and N2B were cloned by polymerase chain reaction with reverse transcription (RT–PCR) from human heart poly(A)$^+$ mRNA (Clontech) using the ThermoScript System (Gibco-BRL). Polyproteins $I27_8$, $I28_8$, $I32_8$, $I34_8$, $I4_8$, $I5_8$ and $I27_3$-N2B-$I27_3$ were constructed using a previously described method based on the identity of the sticky ends generated by *Bam*HI and *Bgl*II restriction enzymes[18,19], and then subcloned into pQE 80L ($I4_8$ and $I5_8$) or pQE 30 ($I27_8$, $I28_8$, $I32_8$, $I34_8$, $I27_3$-N2B-$I27_3$), (Qiagen). $I27_{12}$ was constructed using a non-palindromic *Ava*I restriction site (CTCGGG), as previously described[18]. (I27-PEVK)$_3$ was constructed using a similar method after *Eco*RI ligation of the two domains. (I27-PEVK)$_3$ and I4–I11 were cloned into pET-Ava I (ref. 18) while I27–I34 was cloned in pET 9d (ref. 11). The I27–I34 plasmid was a gift from M. Gautel[11]. This protein has five changes to the sequence published for titin[17]: Thr 42 is replaced by Ala, and Ala 78 is replaced by Thr in the I27 module, Ala 53 is replaced by Thr in the I30 module, there is a deletion that includes the last of two codons of I32 and 87 codons of the I33 domain[18,30], and a deletion of the Glu 89 codon of I34. The cloning strain was SURE-2 (Stratagene). The expression strains used were BL21 (DE3) (I27–I34), BLR (DE3) ($I4_8$, $I5_8$, (I27-PEVK)$_3$), BL21 (DE3) CodonPlus (I4–I11), SURE-2 ($I27_8$, $I27_3$-N2B-$I27_3$), and M15 ($I28_8$, $I32_8$, $I34_8$). Purification of recombinant proteins, from the soluble fraction of the bacterial lysate, was done by Ni^{2+}-affinity chromatography in all the cases but for I4–I11, in which Co^{2+}-affinity purification was used (Clonetech). In the case of (I27-PEVK)$_3$ an additional size-exclusion fast performance liquid chromatography (FPLC) step was used. Proteins were kept at 4 °C in PBS with 5 mM dithiothreitol (DTT) and 0.2 mM EDTA, except for $I27_8$, $I28_8$, $I32_8$, $I34_8$, which were kept in 100 mM imidazole (pH 6.0). All the constructs used in this study have a His-tag at the amino terminus for affinity purification and two Cys residues at the carboxy terminus to promote covalent attachment of the protein to the gold-coated substrate.

AFM

Protein samples (3–10 μl, at a concentration of 10–100 μg ml^{-1}) were deposited onto freshly evaporated gold coverslips to allow the protein to adsorb onto the gold surface. Force–extension measurements were then carried out in PBS saline buffer (137 mM sodium chloride, 2.7 mM potassium chloride and 10 mM phosphate buffer, pH 7.4). The cantilevers are standard Si_3N_4 cantilevers from either Digital Instruments (with a typical spring constant of 100 mN m^{-1}) or TM Microscopes (with a typical spring constant of 12 mN m^{-1}). Every cantilever was calibrated in solution before use.

In situ recording of titin extensibility and force generation

The extensibility of the various I-band titin segments of rabbit cardiac myofibrils were measured using immunoelectron/immunofluorescence microscopy with a set of titin-specific antibodies[6]. Rabbit cardiac muscle expresses almost exclusively the N2B form[16]. Here, the technical names of the antibodies (T12, I17, I18, I20/22, MIR) were replaced for simplicity by consecutive numbers 1 to 5, with 1 being closest to the Z-disk and 5 being located at the A-band/I-band junction (Fig. 3). For each antibody type, the epitope-mobility data obtained over a range of sarcomere lengths (SLs) from 1.8 to 2.8 μm were pooled in SL bins of 50 nm. For each SL bin, the extension of a given titin segment was measured as the distance flanked by two nearest antibody epitopes: proximal Ig region, epitope 1 to epitope 2; N2B, 2 to 3; PEVK, 3 to 4; and distal Ig region, 4 to 5. The epitopes 3 and 4, which measure the extension of PEVK segment, include four additional Ig domains, hence the PEVK extension data were offset by 20 nm. Titin segment extension was then plotted against extension of the entire elastic titin in a half-sarcomere, $x(F)_{\text{I-band}}$, obtained as $x(F)_{\text{I-band}} = (\text{SL} - 1.8\,\mu\text{m})/2$, to account for the functionally stiff titin in the sarcomere (1.6 μm in A-band, 2 × 0.1 μm adjacent to Z-disk). The corresponding stretching force, F, was determined from mechanical recordings of the passive tension of isolated rabbit cardiac myofibrils[6,27] immersed in a buffer solution (6 mM magnesium methanesulphonate, 5 mM dipotassium methanesulphonate, 4 mM Na_2ATP, 15 mM EGTA, with a total ionic strength of 200 mM adjusted with KOH in a 3-N-morpholino-propanesulphonic acid buffer, pH 7.1, 40 μg leupeptin ml^{-1}). Experimental protocols have been described[27]. Passive force was recorded under quasi-steady-state conditions, that is, two to three minutes following a stretch to a new sarcomere length, to exclude viscous and viscoelastic force components that decay during stress relaxation.

Received 5 November 2001; accepted 14 June 2002; doi:10.1038/nature00938.

1. Sigworth, F. J. & Neher, E. Single Na^+ channel currents observed in cultured rat muscle cells. *Nature* **287,** 447–449 (1980).
2. Bustamante, C., Smith, S. B., Liphardt, J. & Smith, D. Single-molecule studies of DNA mechanics. *Curr. Opin. Struct. Biol.* **10,** 279–285 (2000).
3. Smith, D. E. *et al.* The bacteriophage ϕ29 portal motor can package DNA against a large internal force. *Nature* **413,** 748–752 (2001).
4. Finer, J. T., Simmons, R. M. & Spudich, J. A. Single myosin molecule mechanics: piconewton forces and nanometre steps. *Nature* **368,** 113–119 (1994).
5. Lu, H. & Schulten, K. Steered molecular dynamics simulations of force-induced protein domain unfolding. *Proteins Struct. Funct. Genet.* **35,** 453–463 (1999).
6. Linke, W. A. *et al.* I-band titin in cardiac muscle is a three-element molecular spring and is critical for maintaining thin filament structure. *J. Cell Biol.* **146,** 631–644 (1999).
7. Maruyama, K. Connectin/titin, giant elastic protein of muscle. *FASEB J.* **11,** 341–345 (1997).

8. Wang, K. Titin/connectin and nebulin: giant protein rulers of muscle structure and function. *Adv. Biophys.* **33,** 123–134 (1996).
9. Gregorio, C. C., Granzier, H., Sorimachi, H. & Labeit, S. Muscle assembly: a titanic achievement? *Curr. Opin. Cell Biol.* **11,** 18–25 (1999).
10. Trinick, J. & Tskhovrebova, L. Titin: a molecular control freak. *Trends Cell Biol.* **9,** 377–380 (1999).
11. Rief, M., Gautel, M., Oesterhelt, F., Fernandez, J. M. & Gaub, H. E. Reversible unfolding of individual immunoglobin domains by AFM. *Science* **276,** 1109–1112 (1997).
12. Kellermayer, M., Smith, S., Granzier, H. & Bustamante, C. Folding-unfolding transitions in single titin molecules characterized with laser tweezers. *Science* **276,** 1112–1116 (1997).
13. Tskhovrebova, L., Trinick, J., Sleep, J. A. & Simmons, R. M. Elasticity and unfolding of single molecules of the giant muscle protein titin. *Nature* **387,** 308–312 (1997).
14. Tskhovrebova, L. & Trinick, J. Direct visualization of extensibility in isolated titin molecules. *J. Mol. Biol.* **265,** 100–106 (1997).
15. Fisher, T. E., Marszalek, P. E. & Fernandez, J. M. Stretching single molecules into novel conformations using the atomic force microscope. *Nature Struct. Biol.* **7,** 719–724 (2000).
16. Freiburg, A. *et al.* Series of exon-skipping events in the elastic spring region of titin as the structural basis for myofibrillar elastic diversity. *Circ. Res.* **86,** 1114–1121 (2000).
17. Labeit, S. & Kolmerer, B. Titins, giant proteins in charge of muscle ultrastructure and elasticity. *Science* **270,** 293–296 (1995).
18. Carrion-Vazquez, M. *et al.* Mechanical and chemical unfolding of a single protein: a comparison. *Proc. Natl Acad. Sci. USA* **96,** 3694–3699 (1999).
19. Li, H. B., Oberhauser, A. F., Fowler, S. B., Clarke, J. & Fernandez, J. M. Atomic force microscopy reveals the mechanical design of a modular protein. *Proc. Natl Acad. Sci. USA* **97,** 6527–6531 (2000).
20. Li, H. B. *et al.* Multiple conformations of PEVK proteins detected by single-molecule techniques. *Proc. Natl Acad. Sci. USA* **98,** 10682–10686 (2001).
21. Best, R. B., Li, B., Steward, A., Daggett, V. & Clarke, J. Can non-mechanical proteins withstand force? Stretching barnase by atomic force microscopy and molecular dynamics simulation. *Biophys. J.* **81,** 2344–2356 (2001).
22. Marko, J. F. & Siggia, E. D. Stretching DNA. *Macromolecules* **28,** 8759–8770 (1995).
23. Bell, G. I. Models for the specific adhesion of cells to cells. *Science* **200,** 618–627 (1978).
24. Marszalek, P. E. *et al.* Mechanical unfolding intermediates in titin modules. *Nature* **402,** 100–103 (1999).
25. Trombitas, K., Freiburg, A., Centner, T., Labeit, S. & Granzier, H. Molecular dissection of N2B cardiac titin's extensibility. *Biophys. J.* **77,** 3189–3196 (1999).
26. Bueche, F. *Physical Properties of Polymers* 37 (Interscience, New York, 1962).
27. Linke, W. A. *et al.* Towards a molecular understanding of the elasticity of titin. *J. Mol. Biol.* **261,** 62–71 (1996).
28. Higuchi, H., Nakauchi, Y., Maruyama, K. & Fujime, S. Characterization of beta-connectin (titin 2) from striated muscle by dynamic light scattering. *Biophys. J.* **65,** 1906–1915 (1993).
29. Allen, D. G. & Kentish, J. C. The cellular basis of the length-tension relation in cardiac muscle. *J. Mol. Cell Cardiol.* **17,** 821–840 (1985).
30. Scott, K. A., Steward, A., Fowler, S. B. & Clarke, J. Titin; a multidomain protein that behaves as the sum of its parts. *J. Mol. Biol.* **315,** 819–829 (2002).

Supplementary Information accompanies the paper on *Nature*'s website (http://www.nature.com/nature).

Acknowledgements

We thank H. Erickson for the electron microscope pictures of I27 polyproteins. W.A.L. thanks the German Research Foundation for a Heisenberg fellowship. This work was supported by the National Institutes of Health (J.M.F.)

Competing interests statement

The authors declare that they have no competing financial interests.

Correspondence and requests for materials should be addressed to J.M.F. (e-mail: jfernandez@columbia.edu).

Supplementary Information

1.- Protein engineering and single molecule AFM recordings.

Single-molecule mechanical recordings were made using the method originally described by Rief et al[1]. In our experiments, recombinant proteins are placed on the surface of a gold covered coverslip where they can be picked up by an AFM tip. All proteins used were constructed as polyproteins following the methods first described by Carrion-Vazquez et al[2] and Li et al[3]. When a polyprotein is picked up and stretched, the resulting force-extension curve has the characteristic appearance of a sawtooth pattern. The sawtooth pattern results from the sequential unfolding of all the protein modules, as the protein is elongated[2] (Figure 1). Several characteristic features of a sawtooth pattern are revealing of the mechanical architecture of the protein module being studied. For example, the peak force reached before an unfolding event measures mechanical stability[3]. The force-extension trace preceding an unfolding event can reveal mechanical intermediates[4]. Other experimental protocols such as double pulse experiments, can measure folding rate[2]. Varying the rate of pulling will result in sawtooth patterns of different amplitude, which can be used to estimate the distance between the native state and the transition state[2]. We used all these protocols to characterize the mechanical design of the four regions of human cardiac I band titin.

In AFM experiments it is important to ensure that only data from single molecules is taken into account, since the mechanical features will scale with the number of molecules that are picked up. The use of polyproteins in these experiments is essential, because they can be recognized by their mechanical fingerprint; the sawtooth pattern. A sawtooth pattern clearly identifies a single molecule. If the AFM tip picks up more than one molecule, the resulting force-extension curve will show superimposed sawtooth patterns.

In addition to identifying single molecules, the sawtooth pattern fingerprint of a polyprotein can be used to provide certain identification of protein regions of very low mechanical stability[5, 6]. For example, cardiac titin possesses two regions of unknown structure, the N2B region and the PEVK region. Both regions have been proposed to be random coils. These regions pose a particular problem for AFM studies because upon stretching, a random coil would give a featureless force extension curve. Lacking a clear mechanical fingerprint we cannot identify the molecule being pulled or be sure if it is a single molecule. This problem is of particular importance in the case of random coils because the flexibility of the random coil, scales linearly with the number of molecules that are placed in parallel[5]. Hence, it is essential to ensure that the mechanical measurements of these suspected random coil regions are done on single molecules. We solve this problem by engineering proteins containing the unknown region plus multiple repeats of the I27 titin module. We use the I27 module in these designs because its mechanical unfolding has been characterized in detail and can be easily recognized[2] . The design principle behind these polyproteins considers that the modules are independent of each other, and that they will unfold following their mechanical stability[3] . When stretching a polyprotein that contains the stable I27 module together with a random coil, we expect that the random coil will extend first and that the last events will be the unfolding of the I27 modules.

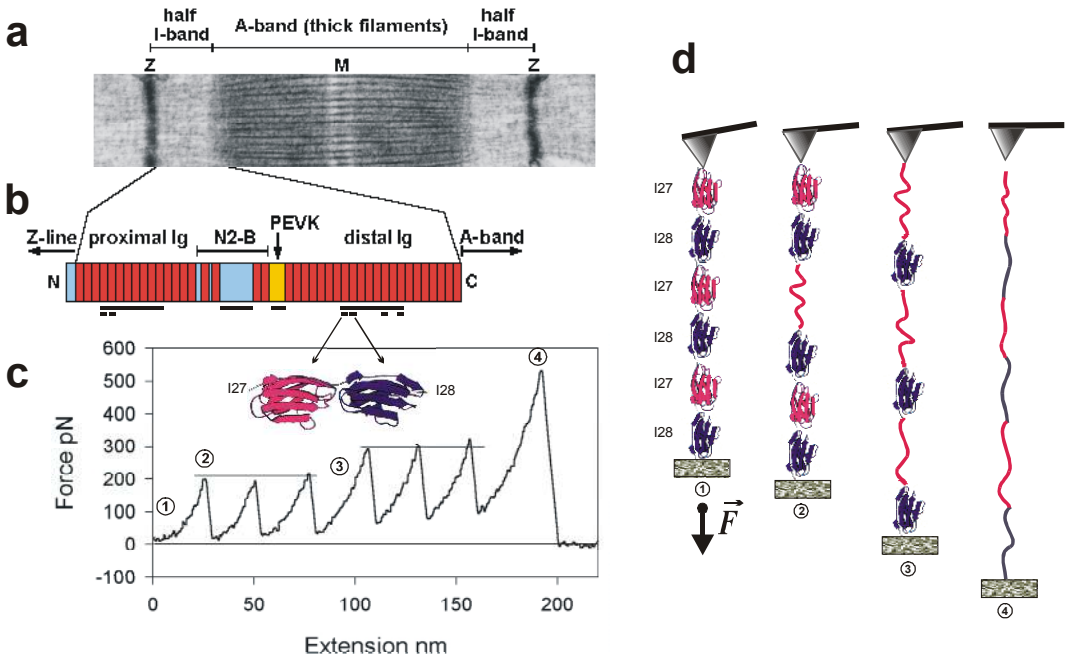

Figure 1. Experimental approach to study the elastic region of titin. **a)** Electron micrograph of a cardiac muscle sarcomere; titin molecules span from the Z-disk (Z) to the M-line (M). **b)** Modular structure of the elastic I-band section of the human cardiac N2B-titin isoform. Color coding: red-Ig domains; blue-unique sequences; yellow-PEVK domain. Horizontal bars: positions of the engineered proteins used in this study. **c)** Force vs. extension curve for a heterodimer polyprotein containing three copies each of Ig-domains I27 and I28. Stretching this polyprotein resulted in force-extension curves with equally spaced force peaks but two distinct levels of unfolding forces, ~ 200 pN and ~300 pN. The last force peak corresponds to the detachment of the protein from the AFM tip. **d)** Schematic of AFM-aided stretching and unfolding of the $(I27\text{-}I28)_3$ heteropolyprotein. Numbers ①-④ correspond to the stages marked in c). ① shows the polyprotein adsorbed to an AFM tip and straightened out; ②-④ indicate that stretching the protein increases the applied force on the domains, causing unfolding of the weak domains (I27) followed by unfolding of the mechanically stronger domains (I28), before the fully unfolded polypeptide detaches from the AFM tip (④).

2.- The flexibility of the tandem Ig regions.

The elasticity of the folded Ig region is thought to result from the bending of the domain linkers joining the folded immunoglobulin domains. From this point of view, the tandem Ig regions behave like a rigid random coil. It would seem relatively straightforward to estimate the persistence length of a folded tandem Ig region by fitting the WLC to the force-extension curve that precedes any unfolding event. However, the WLC equation that is commonly used in single molecule AFM experiments[7], is an approximation of the WLC model that is accurate only when the persistence length is

much smaller than the contour length[7]. However, this is likely not true for a folded $I27_{12}$ polyprotein with a short contour length of 58 nm and a persistence length that should be at least the size of a single folded Ig domain (4.4 nm). Hence, we cannot use the WLC approximation[7] under these conditions. An estimate of the persistence length of a folded polyprotein can be obtained from electron micrographs of single polyproteins. Figure 2 shows a rotary shadowed electron micrograph of the $I27_{12}$ polyprotein. The picture shows single proteins that bend in random directions. We measure the contour length, L_c, of each protein (yellow trace in Figure 2A, left panel) and their end-to-end length x (red trace in Figure 2A, left panel). Ideally the $I27_{12}$ polyproteins all have the exact same length, however, during protein expression and purification there is some truncation (Figure 2A, right panel) that makes the chains shorter and also there is some dimer formation through the formation of disulphide bonds between pairs of polyproteins, through the two C-terminal Cys engineered into the sequence. These variations in length can be readily observed in the E.M. picture giving a range of contour lengths between 20-70 nm (see Figure 2A, left panel). Models of polymer elasticity have predicted that when a polymer is in thermal equilibrium, its end to end length will follow a Gaussian distribution. Indeed, molecules of similar contour lengths, L_c, have widely varying values of x which follow a Gaussian distribution (not shown). The expected value of the end-to-end length $\langle x \rangle$, is related to the contour length of the polymer chain, L_c, and the flexibility of the polymer, measured by its persistence length p, following the 2D-equilibrium model[8]:

$$\langle x^2 \rangle = 4pL_c\left(1-\left(\frac{2p}{L_c}\left(1-e^{\frac{-L_c}{2p}}\right)\right)\right) \qquad (1)$$

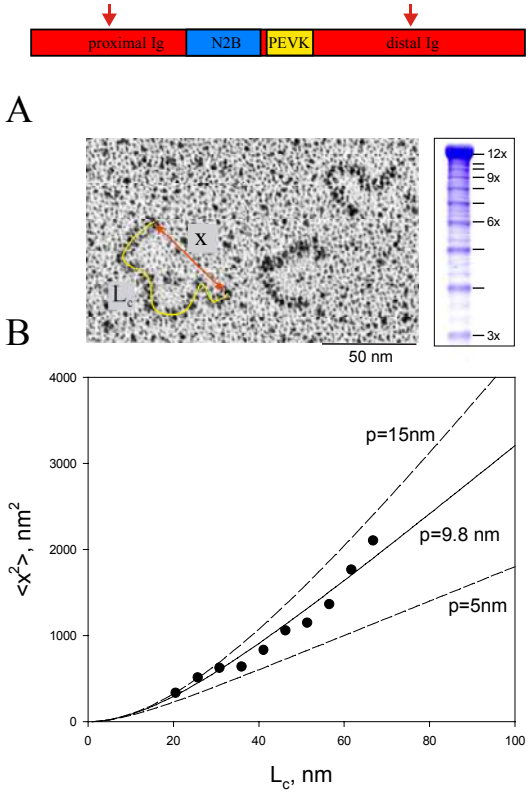

Figure 2. Flexibility of a folded tandem Ig protein. A, left panel) Rotary shadowed electron micrograph showing individual $I27_{12}$ polyproteins (micrograph courtesy of Dr. Harold Erickson). The polyproteins appear as randomly bent rods of varying contour length L_c. The observed variations in the contour length of the polyprotein are likely to be due to truncation (right panel). The yellow line indicates the measured contour length, L_c, the red line the measured end-to-end distance, x. **A, right panel)** Coomassie blue staining of an 8% SDS-PAGE gel from the $(I27)_{12}$ polyprotein after affinity purification. It shows a major band corresponding to the full-length polyprotein and also a ladder of smaller molecular weight proteins, which are multiples of the size of the I27 monomer. (**B)** Plot of the square of the average end-to-end distance as a function of the contour length (filled circles, data obtained from 245 individual molecules). The solid line is a nonlinear fit of equation 1, giving a value of p=9.8 ±0.6 nm. The dashed lines correspond to fits of p=15 nm and p=5 nm.

Hence, by plotting $\langle x^2 \rangle$ vs L_c we can use this equation to extract the value of the flexibility of the folded $I27_{12}$ polyprotein. Figure 2 shows a plot of $\langle x^2 \rangle$ vs L_c where the experimental data (circles) are compared with a plot of equation (1) at three different values of persistence length (p = 5, 9.8 and 15 nm). The data is best fit by p = 9.8 nm and we take this as the value of the flexibility of the folded $I27_{12}$ polyprotein. This value is similar to that obtained by Tskhovrebova and Trinick[9] for skeletal titin using E.M. techniques (p=13.5±4.5nm) and also similar to the value by Higuchi et al.[10] in dynamic light scattering studies on titin (p=15nm). We expect that a value of p=9.8 nm also applies to the rest of the folded tandem immunoglobulin regions. We also fit the data (not shown) with the so-called trapping model[8]. However, in this case we get p~ 50 nm, which is unreasonably large because it is comparable to the contour length of the molecule.

3.- The effect of module unfolding on titin elasticity.

What would happen to the elasticity of titin if an immunoglobulin module unfolds? As predicted by the WLC model, the change in force (ΔF) generated by small extensions (Δx) of a protein gives an elastic modulus of $\frac{\Delta F}{\Delta x} \cong \frac{3kT}{2pL_c}$ where p is the persistence length and L_c is the contour length of the protein. This linear relationship between force and extension is valid only for small extensions such that $\Delta x << L_c$. Module unfolding has two important effects. It increases the protein's contour length and therefore the range over which the protein can be extended. Unfolding also causes a large decrease in persistence length, from that of a rigid chain of folded modules (p ~ 10 nm, Figure 2) to a more flexible extended chain (p~0.6 nm). Hence, unfolding may serve to regulate the stiffness of the tandem modular regions.

In the simplest case, unfolding can be modeled by a two state reaction between the native and the unfolded state, $N \leftrightarrow U$. The rate constants between these states are force dependent and given by $\alpha=\alpha_0 exp(F\Delta x_u/k_BT)$ and $\beta=\beta_0 exp(-F\Delta x_f/k_BT)$, where α_0 is the unfolding rate constant at zero force and β_0 is the folding rate constant at zero force[36]. At a constant force F, the probability of unfolding is given by $P_u(F) = \frac{\alpha}{\alpha+\beta}$. The unfolding of the I27 immunoglobulin module has been studied in detail using single molecule atomic force microscopy. In the absence of an applied force the probability of unfolding is very low, $P_u^{I27}(0) = 0.0003$, whereas if only 13.7 pN are applied, the steady state probability of unfolding grows by about 1000 fold to $P_u^{I27}(13.7) = 0.5$.

4.- Steered Molecular Dynamics. The structure of I1 and I27 was solvated and equilibrated with CHARMM22 (ref. 11) force field following the procedure described in reference 12. The forces were applied along the line connecting the N- and C- termini. Simulations were done with the molecular dynamics program NAMD[13] on a parallel LINUX cluster with 18 nodes. Simulation time: 1 ns for each force applied. The trajectories were recorded every picosecond and analyzed with program VMD[14].

5.- Structural basis of unfolding intermediates.

The structure of only two immunoglobulin modules from the cardiac I band is currently available, the I1 module from the proximal region[15] and the I27 module from the distal region[16]. Figure 3A,B shows the 3-D structure of the I1 and I27 modules respectively. Both domains form similar β–sandwiches with 4 β-strands in each sheet. The backbone hydrogen bonds attaching the A' and A β-strands to the remainder of the fold are marked as thick orange traces. For the I27 module, these bonds were singled out to be the origin of both, the unfolding intermediate (the two H-bonds between the A and B β-strands[4] and the main barrier to complete unfolding (the six H-bonds between the A' and B β-strands[4, 17]). By contrast we now find that the mechanical design of I1 is different. Although I1 also has 6 H-bonds between the A' and G β-strands, it possesses 6 hydrogen bonds between the A and B β-strands, versus only two in the I27 module. Assuming that the I1 module is representative of the proximal immunoglobulin domains, the relative strengthening of the attachment between the A and B β-strands may be the basis for the lack of an unfolding intermediate in the proximal tandem Ig region.

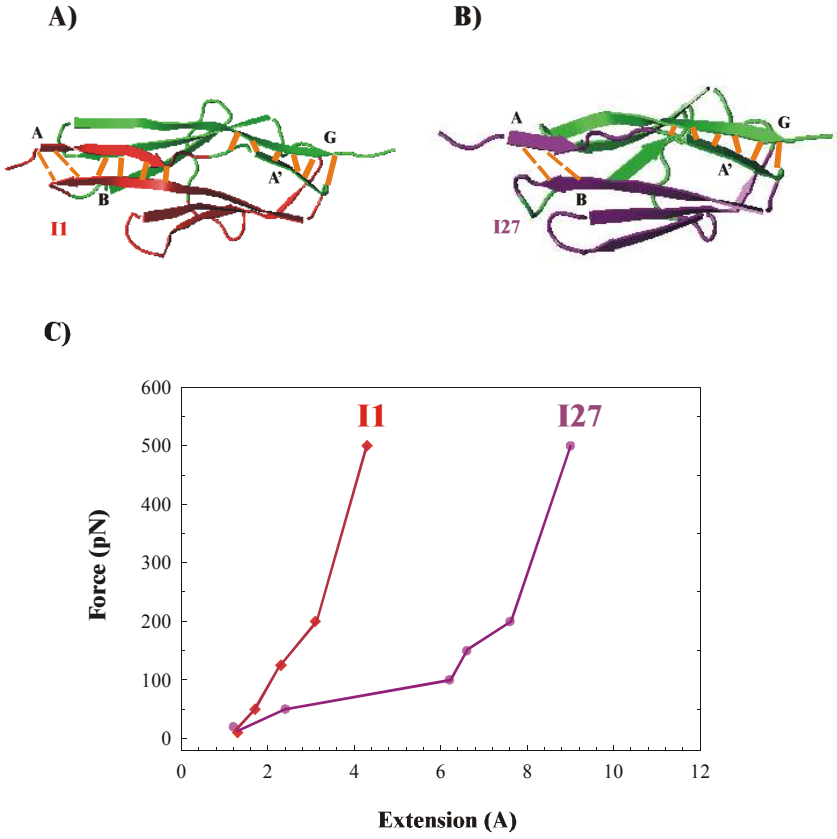

Figure 3. Molecular Dynamics simulations of the extension of a proximal (I1) and a distal (I27) immunoglobulin domain of I band titin. A) and B) show the simulated extension of the I1 and I27 titin modules, stretched by a constant force of 200 pN. At this force, the H-bonds binding the A and B β-strands of I1 are largely intact, whereas for the I27 module the A and B strands have already separated, allowing for a small extension and creating an intermediate state of unfolding. C) A plot of the simulated end-to-end extension of the I1 and I27 modules at stretching forces ranging from 0-500 pN. The

unfolding intermediate in I27 is evident as the discontinuous elongation that is observed at ~ 100 pN. By contrast, I1 does not show such an intermediate because of the presence of six H-bonds linking the A and B β-strands.between the A and B β-strands and the separation of these strands[4]. In the case of I1, for stretching forces below 200 pN, all H-bonds between the A and B β-strands remain formed. At 200 pN the first 2 H-bonds break, but as the other four hydrogen bonds remain intact, AB strands do not separate, which limits the domain extension to 3 Å range. Stretching at much higher forces will trigger the simulated unfolding of both the I1 and the I27 modules. The main energy barrier to unfolding of the I27 module is the rupture of the six H-bonds between the A' and G β-strands[12, 17]. By contrast, the main energy barrier for the unfolding of I1 corresponds to the rupture of the six H-bonds between the A and B β-strands (Klaus Schulten, personal communication). It is clear then, that I1 can unfold without a significant unfolding intermediate in an all-or-none fashion.

SMD simulations of the extension of I1 under a constant stretching force ranging between 10 and 500 pN, confirm this view. Figure 3C shows that within this force range I1 deforms slightly, in a linear fashion by up to 3 Å at 200 pN. By contrast, extension of the I27 module is discontinuous at ~100 pN with the extension reaching 8 Å at 200 pN (Fig. 3C). We have previously identified this discontinuous extension of the I27 module as an unfolding intermediate which is caused by the breakage of the 2 hydrogen bonds

6.- Reconstitution of titin elasticity based on the WLC polymer elasticity model.

The WLC model of polymer elasticity is approximated by the following equation (ref. 7).

$$F_{WLC}(x,p,L_c)=\frac{kT}{p}\cdot\left(\frac{1}{4}\left(1-\frac{x}{L_c}\right)^{-2}-\frac{1}{4}+\frac{x}{L_c}\right) \qquad (2)$$

where L_c is the contour length, and p is the persistence length. This approximation to the WLC model is commonly used to fit the single molecule AFM data. Titin elasticity can be reconstructed using the FJC model as described in the main text (equations 3-6). A similar reconstruction of titin elasticity based on the WLC approximation is presented here (Fig. 4).

We calculate the extension of each segment at a given force: $x(F)_{N2B}$ and $x(F)_{PEVK}$ by setting p_{N2B}=0.66 nm, p_{PEVK}=0.91 nm, $L_c^{N2B}=217\ nm$ *and* $L_c^{PEVK}=68\ nm$ (see table I), and then calculating $x_{N2B}(F)=F_{N2B}^{-1}(x,0.66,217)$ and $x_{PEVK}(F)=F_{PEVK}^{-1}(x,0.91,68)$ where the -1 sign on the function denotes the numerical inversion of equation 2, to find x(F).

The extensibility of the proximal and distal tandem Ig domain segments, $x(F)_{proximal}$ and $x(F)_{distal}$, are calculated in a similar way, however, in this case, the contour length, L_c, and the persistence length, p, depend on module unfolding [see main

text]. Thus, the extension of the proximal Ig region under an applied force, $x(\mathrm{F})_{\mathrm{proximal}}$, is fully described by:

$$x(F)_{proximal} = F^{-1}\left(x, p^{folded}, L_c^{folded}\right) + F^{-1}\left(x, p^{unfolded}, L_c^{unfolded}\right) \quad (2)$$

and the remainder of the computation of $X_{\text{I-band}}(F)$ is done as described by equations 4-6 of the main text. The results of these calculations are shown in Figure 4. The Figure shows that the extension of each I band segment as well as the force-extension relationship for a single myofibril can be predicted reasonably well.

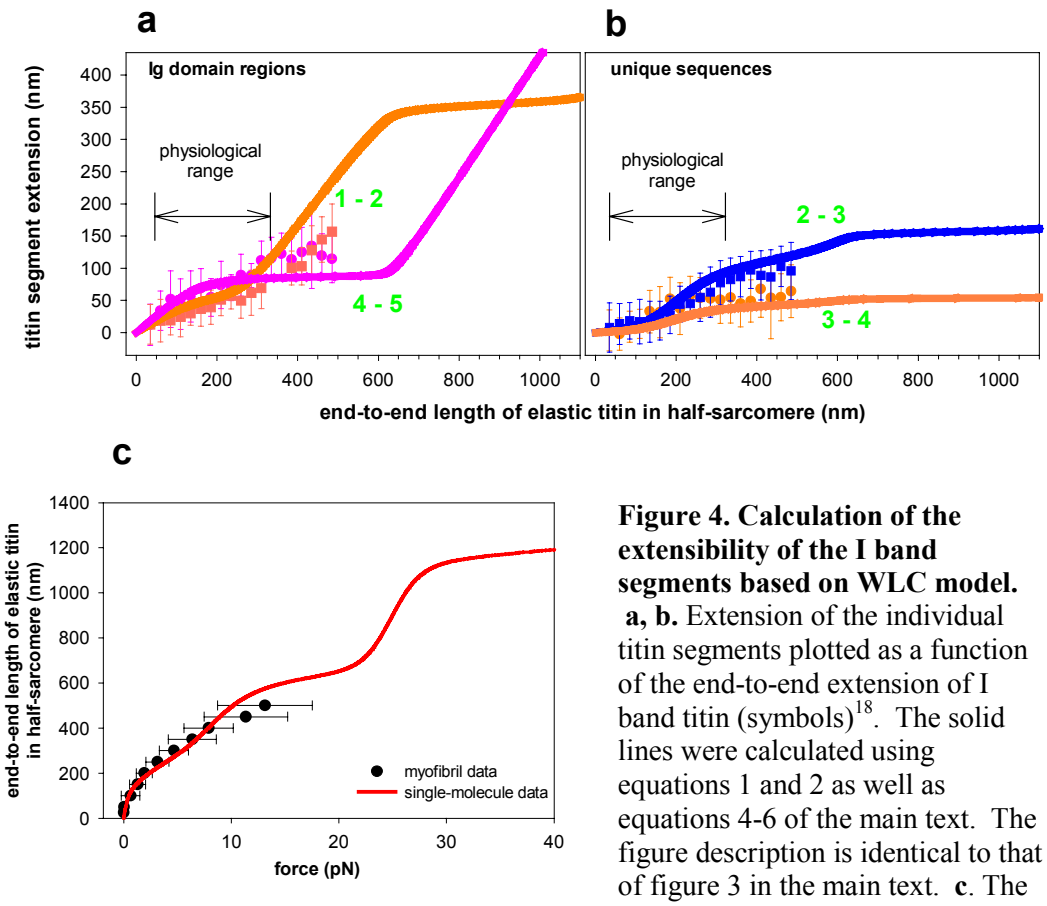

Figure 4. Calculation of the extensibility of the I band segments based on WLC model. **a, b.** Extension of the individual titin segments plotted as a function of the end-to-end extension of I band titin (symbols)[18]. The solid lines were calculated using equations 1 and 2 as well as equations 4-6 of the main text. The figure description is identical to that of figure 3 in the main text. **c**. The WLC based calculation (solid line) also predicts the passive force-extension relationship of single cardiac myofibrils (Symbols). The scaling factor used here is 4×10^9 titins per mm^2 of cross-sectional area.

References

1. Rief, M., Gautel, M., Oesterhelt, F., Fernandez, J. M. & Gaub, H. E. Reversible unfolding of individual immunoglobin domains by AFM. *Science*, **276**, 1109-1112, (1997).
2. Carrion-Vazquez, M., Oberhauser, A. F., Fowler, S. B., Marszalek, P. E., Broedel, S. E., Clarke, J. & Fernandez, J. M. Mechanical and chemical unfolding of a single protein: a comparison. *Proc. Natl. Acad. Sci. USA,* **96**, 3694-3699 (1999).
3. Li, H. B., Oberhauser, A. F., Fowler, S. B., Clarke, J., and Fernandez, J. M., Atomic force microscopy reveals the mechanical design of a modular protein. *Proc. Natl. Acad. Sci. U. S. A.*, **97**, 6527-6531 (2000).
4. Marszalek, P. E., Lu, H., Li, H. B., Carrion-Vazquez, M., Oberhauser, A. F., Schulten, K. & Fernandez, J. M. Mechanical unfolding intermediates in titin modules. *Nature*. **402**, 100-103 (1999).
5. Li. H. B., Oberhauser, A. F., Redick, S. D., Carrion-Vazquez, M., Erickson, H. P. & Fernandez, J. M. Multiple conformations of PEVK proteins detected by single-molecule techniques. *Proc Natl Acad Sci U S A.* **98**, 10682-10686 (2001).
6. Best, R. B., Li, B., Steward, A., Daggett, V. and Clarke, J. Can non-mechanical proteins withstand force? stretching barnase by atomic force microscopy and molecular dynamics simulation. *Biophys J.* **81**, 2344-2356 (2001).
7. Marko, J. F. & Siggia, E. D. Stretching DNA. *Macromolecules*, **28**, 8759-8770 (1995).
8. Rivetti, C., Guthold, M. & Bustamante, C. Scanning force microscopy of DNA deposited onto mica: equilibration versus kinetic trapping studied by statistical polymer chain analysis. *J. Mol. Biol.* **264**, 919-932 (1996).
9. Tskhovrebova L & Trinick J. Flexibility and extensibility in the titin molecule: analysis of electron microscope data. *J. Mol Biol* **310**(4):755-771(2001).
10. Helmes M, Trombitas K, Centner T, Kellermayer M, Labeit S, Linke WA & Granzier H. Mechanically driven contour-length adjustment in rat cardiac titin's unique N2B sequence: titin is an adjustable spring. *Circ Res.,***84**(11):1339-1352. (1999).
11. Brooks, B., Bruccoleri, R., Olafson, B., States, D., Swaminathan, S. & Karplus, M. CHARMM: A program for macromolecular energy, minimization, and molecular dynamics calculations. *J. Comp. Chem.* **4**, 187-217 (1983).
12. Lu, H., Isralewitz, B., Krammer, A., Vogel, V. & Schulten, K. Unfolding of titin immunoglobulin domains by steered molecular dynamics simulation. *Biophys. J.***75**, 662-671 (1998).
13. Nelson, M., Humphrey, W., Gursoy, A., Dalke, A., Kale, L., Skeel, R., & Schulten, K. NAMD – A parallel, object-oriented molecular dynamics program. *J. Supercomputing App*. **10**, 251-268 (1996).
14. Humphrey, W., Dalke, A., & Schulten, K. VMD – Visual Molecular Dynamics. *J. Mol. Graphics*, **14**, 33-38 (1996).
15. Mayans, O., Wuerges, J., Canela, S., Gautel, M. & Wilmanns, M. Structural Evidence for a Possible Role of Reversible Disulphide Bridge Formation in the Elasticity of the Muscle Protein Titin. *Structure* **9**, 331-340 (2001).
16. Improta, S., Politou, A., & Pastore, A. Immunoglobulin-like modules from titin I-band: extensible components of muscle elasticity. *Structure*, 4, 323-337 (1996).

17. Lu, H. & Schulten, K. The key event in force-induced unfolding of titin's immunoglobulin domains. *Biophysical Journal* **79**, 51-65 (2000).
18. Linke, W. A., Rudy, D.E., Centner, T., Gautel, M., Witt, C., Labeit, S.& Gregorio, C.C. I-band titin in cardiac muscle is a three-element molecular spring and is critical for maintaining thin filament structure. *J. Cell Biol*. 146, 631-644, (1999).